Landscape and Ecological Engineering (2025) 21:133–150
https://doi.org/10.1007/s11355-024-00628-3

ORIGINAL PAPER

Multi-dimensional analysis of land use/land cover and urbanization on seasonal variation of land surface temperature in İzmir, Türkiye

Oznur Isinkaralar[1] · Kaan Isinkaralar[2] · Dilara Yilmaz[3] · Sevgi Öztürk[1]

Received: 11 May 2024 / Revised: 9 August 2024 / Accepted: 26 October 2024 / Published online: 9 November 2024

Abstract
Climate change-induced extreme meteorological phenomena, such as sudden temperature fluctuations, are raising global concerns. Increasing their adaptation capacity against temperature changes between seasons is becoming a more critical issue. The aim of this paper is to explore the association between surface temperature (ST) during the four seasons and urban geography in the city center of Izmir. The study identifies built environment parameters that impact seasonal land surface temperatures (LST) through spatial and statistical analysis at the local scale. At the same time, QUADRANT analysis revealed the spatial distinction between neighborhoods showing high LST compliance on a local scale (cooler summers and warm winters as well as neighborhoods showing LST sensitivity (hotter summers and colder winters. A spatial distinction is also revealed, showing significant differences in vegetation, number of buildings, building heights, and land use/cover change types. Geographic regression simulations show that the density of vegetation is vital in mitigating seasonal LST values, especially in making summers cooler and winters warmer. At the same time, population and built-up area density also play a role in increasing LST. Findings are consistent for neighborhood-scale analyses. Variables explain 26% in autumn, 31% in winter, 34% in spring, and 43% in summer. The study, which reveals the pressure of population and urbanization on temperatures, also highlights the adaptive character of the environment in adjusting the temperatures.

Keywords Climate policy · Spatial modeling · Adaptation strategies · Moran I · Urban heat island

Abbreviations

AICc	Akaike's information criterion
CC	Climate change
GWR	Geographically weighted regression
GW	Global warming
HW	Heat waves
LSA	Land surface albedo
LST	Land surface temperature
LULC	Land use/land cover
NDVI	Normalized difference vegetation index
OLS	Ordinary least squares
SS	Statistically significant
S	Summertime
ST	Surface temperature
UHI	Urban heat island
UM	Urban morphology
W	Winter season
WHO	World health organization

✉ Oznur Isinkaralar
obulan@kastamonu.edu.tr

[1] Department of Landscape Architecture, Faculty of Engineering and Architecture, Kastamonu University, 37150 Kastamonu, Türkiye

[2] Department of Environmental Engineering, Faculty of Engineering and Architecture, Kastamonu University, 37150 Kastamonu, Türkiye

[3] Department of Landscape Architecture, Graduate School of Natural and Applied Sciences, Kastamonu University, 37150 Kastamonu, Türkiye

Introduction

Although rapid urbanization provides social and economic development, it also causes many social and ecological problems to arise in cities (Wu et al. 2010). One of the most important of these problems is urban heat island (UHI) formation. During the urbanization process, natural surfaces are turned into permeable covers. Therefore, this implies that the land surface temperature (LST) to increase (Imran et al. 2021). Extremely high temperatures exacerbate many types of environmental issues, including the UHI effect and extreme climate phenomena, especially in metropolitan cities, causing people to be negatively affected physically and psychologically (Wang et al. 2021; Yang et al. 2021; Ren et al. 2022; Xin et al. 2022).

Global warming (GW) and climate change (CC) worldwide are causing more extreme weather occurrences (Aydin et al. 2024; Guven et al. 2024). Climate norms caused by GW have had an impact on cities and people in various ways, including meteorological droughts that have occurred in cities since 1974, heat waves (HW) in early summer that occur in spring, and cold solid waves in autumn (Park and Song 2023). According to the Intergovernmental Panel on Climate Change (IPCC), around 250,000 people are estimated to be dead annually from 2030 to 2050 because of CC (IPCC 2023). Considering that urbanization will continue, increasing temperatures is inevitable for cities. Therefore, it is essential to develop strategies requiring effective, appropriate mitigation measures and environmental adaptation during the CC process (Isinkaralar et al. 2024a).

Increasing urbanization, especially anthropogenic activities greatly affects the climate worldwide (WHO 2014; Hornsey and Fielding 2020). This situation has also caused and will continue to cause major changes in the physical geography of cities (IPCC 2022). Rapid population growth in cities causes natural areas such as vegetation, water bodies, and agricultural areas to turn into impermeable surfaces and urban infrastructure areas (Yao et al. 2017; Dai et al. 2018). With the continuous increase in urbanization, the urban population also increases. Therefore, LULC plays a vital role in LST change (Choudhury et al. 2019; Tan et al. 2020; Ayanlade et al. 2021).

Urbanization and rapid population growth in recent years have further increased the formation of UHI. The unplanned and unequal expansion of cities also causes an unbalanced increase in temperatures (Yin et al. 2018; Tanoori et al. 2024). Therefore, LST is widely used to characterize the relationship between UHI formation and LULC, 3D urban geometry features (Oke et al. 2017; Guo et al. 2020a; Zhou et al. 2022; Liu et al. 2023). These relationships at the urban scale vary depending on seasonal and spatial characteristics and population density (Song et al. 2020; Guo et al. 2023). To reduce UHI formation in urban climate studies, determining the homogeneity and heterogeneity of local morphology also appears as an crucial requirement. (He et al. 2019a; Yuan et al. 2024). In urban environments, LST is an essential parameter in determining surface temperature (ST). Urban elements such as buildings and roads significantly affect temperatures (Liu et al. 2022; Moazzam et al. 2022). Therefore, determining and analyzing urban elements and their effects on thermal conditions are fundamental steps in sustainable urban design (Boeing 2018; Zhao et al. 2023a, b). Urban form analyses also enable cities to improve their capacity to adapt to extreme temperatures. Therefore, understanding urban form factors, which are closely related to LST changes throughout urban areas and seasons, is vital in urban climate studies. With seasonal changes, it will also be easier to create more effective policies in the adaptation process to climate change (Isinkaralar et al. 2024b).

UHI and HW are among the issues which will become more prevalent in cities in the Mediterranean basin, one of the major flashpoints of the climate crisis, in the future due to the harmful impacts of CC. According to climate change projections and the IPCC, in addition to temperature increases, it is necessary to pay attention to sea level increases, which may cause changes in many aspects of cities. Especially in coastal cities such as Izmir and Istanbul, due to their population density, socio-economic development, and economic importance as commercial centers, it is predicted that the increase in sea levels may cause extreme storm events in cities and that these events will cause many physical, environmental and, therefore, social problems in cities. It is also predicted that these problems in cities will increase the formation of UHI and therefore the resilience of cities in the climate change process will weaken. According to the 6th Assessment Report published by the IPCC, the most pessimistic scenario is estimated to rise by approximately 0.5 m by the middle of the century and decreased by about 1 m until late in the century (IPCC 2022). Rising sea levels will cause extreme storm events in these cities and will cause many physical, environmental, and social problems. It is crucial to produce the most effective solutions against this process, which is expected to cause significant changes in the coastline. One of the main objectives is to increase the intervention power of cities in the adaptation process to climate change, which is one of the main causes of vital environmental problems today. In this context, this research emphasizes the relationship between ST and morphological features that can be intervened during four seasons at the neighborhood scale in Konak district of Izmir and the built environment parameters that affect this relationship.

Literature review

The determinants of LST, which represent the UHI, have been studied with variables and procedures in regions with varying regional and geographical specificities. While some of the studies used geographic information systems-based methods by Bokaie et al. (2016), He et al. (2019b), and Guo et al. (2020b). Similarly, Guo et al. (2021) used to investigate regional and geographical data with ordinary least squares (OLS) and geographically weighted regression (GWR). However, some of them used calculation methods based on remote sensing-based spectral indices by Firozjaei et al. (2018), Lu et al. (2020), and Zhang et al. (2023). The UM has generally been accepted as the main factor affecting UHI in studies

(Dimoudi and Nikolopoulou 2003; Li et al. 2011; Elmes et al. 2017; Estoque et al. 2017; Zhou et al. 2018).

In addition to these evaluations, developments in geospatial analytics have enabled the evaluation of complex urban geometries in particular within the scope of 3D features. With these developments, an increasing number of studies in recent years have investigated the relationship between urban morphology and UHI in the context of climate change and urbanization (Deilami et al. 2018; Nastran et al. 2019). However, most studies do not take into account the temporal and spatial changes in UHI formation and its relationship with urban morphology. Another critical situation that stands out in the studies is that UHI impacts not only affect urban climate and human health but also increase energy consumption (Weng et al. 2004; Yuan and Baurer 2007) and pollutant emissions (Adams and Smith 2014) that threaten urban sustainable development (Shiflett et al. 2017; Liu et al. 2021). With rapid urbanization, the number of people living in cities is increasing, and available land resources are decreasing. Therefore, UM constantly changes (Estoque and Murayama 2014; Meng et al. 2018; Sun et al. 2020a). Studies generally focused on determining the effects between LST and LULC or UM at the urban or local scale. However, especially in coastal cities at the neighborhood scale, there is no study comparing the relationship between environmental, physical–social factors such as LST, LULC, average age, population density, total number of buildings, average building height, transportation network in the same model and also according to seasonal differences.

Another important finding in the studies is that urban climate should be addressed with a holistic perspective from the local to the regional scale. Planning decisions made as a result of evaluations made at the local scale, especially at the neighborhood scale, and land use decisions made at the regional scale are largely effective on urban climate. UHI studies conducted at the neighborhood scale emphasize that determining the effects of various land features on UHI and its relationship with the spatial scale are of critical importance for creating sustainable and healthy cities (Ferwati et al. 2019; Parsaee et al. 2019; Shi et al. 2021; Qi et al. 2024; Martin et al. 2024).

In this context, the research questions are as follows: (1) how can the relationship between LST and UM be modeled seasonally? (2) what are the key parameters for climate-sensitive sustainable urban development policies that can be produced based on the impact of UM on LST at the neighborhood scale?

Materials sand methods

Study area

Izmir is located in the south of Türkiye, between 38° 25′ 60″ northern latitudes and 27° 9′ 0″ eastern longitudes. The province's surface area is 12,012 km^2, and its sea level rise is 2 m. Izmir is located at the beginning of a long and narrow bay. Konak, one of the central districts of Izmir, was selected as the field of investigation in Fig. 1. The surface area of Konak district is 24 km^2. The district has a total of 113 neighborhoods, and its total population is 332,277 people, according to Turkish Statistical Institute (TUIK) 2022. Konak district, one of the metropolitan districts of Izmir, has many social, cultural, and economic values and is among the most important tourism cities in Türkiye.

Konak district is in the subtropical climate zone and Csa class according to the Köppen climate classification. The region has a Mediterranean climate, with mild and rainy winters and hot and dry summers. Annual precipitation varies between 300 and 700 mm. In the study area, strong winds are seen from December to April, while calm winds are seen from June to October. The wind mostly blows from the southwest to the northeast.

Data sources and processing

The current paper aimed to determine the association existing between ST and UM in the CC process and to compare this relationship depending on seasonal parameters. In this context, LST, an essential component of LST, was determined as the dependent variable. In contrast, 16 independent variables representing the UM and population component were determined in Table 1.

Land surface temperature (LST)

The LST map was obtained from 4 Landsat 8 OLI/TIRS satellite pictures supplied by the United States Geological Survey (USGS) with a resolution of 30*30 m and representing the study area in four seasons. The climate characteristics of Konak district effectively determined each period of satellite imagery. Since the Landsat satellite passes over Izmir city at certain hours, images belonging to 08:45 in the morning were used. The clearest and smoothest satellite images were selected by considering the resolution status and cloudiness rates of the images. Since there are some software distortions in the satellite images, only one-day LST was used in seasonal ST determination. Satellite images within this scope were used to represent the winter season on 07.01.2023, 07.11.2023 to the autumn season, 07.06.2023 to the spring season, and 09.07.2023 to the summer season. The algorithms used to make the LST map with the help of the ArcGIS 10.4.1 program are here below (Barsi et al. 2014; Roy et al. 2020). Equation 1 was initially applied to the data from band 10 of the Landsat 8 OLI satellite view to convert them into the spectral radiance values:

Fig. 1 Maps of the working site

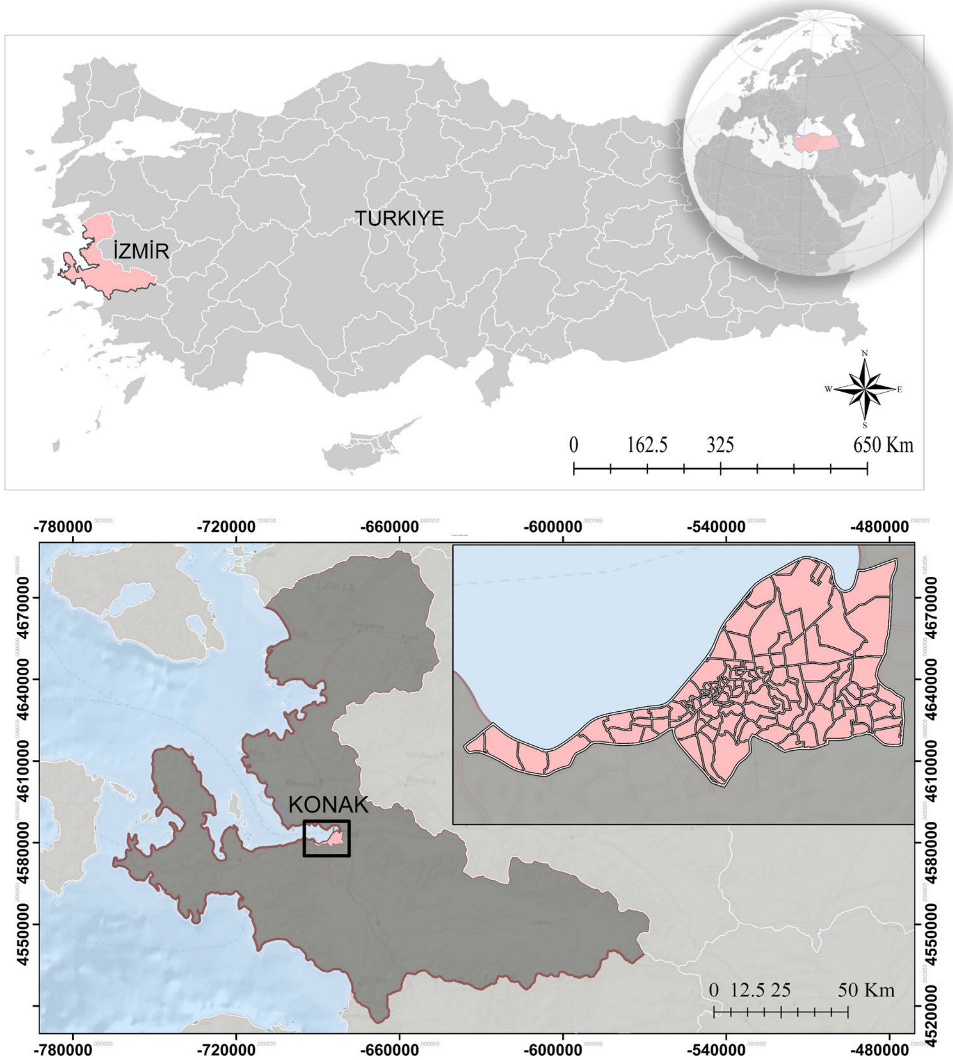

$$L_\lambda = ML * Qcal + AL \quad (1)$$

where Lλ, ML, AL and Q_{Cal} are the TOA spectral luminance (Watt/(m^2 × srad × m)), Radiance Mult Band (Band10), Radiance Add Band(10) from the brightness values of the images, and quantized and calibrated standard product pixel values as Band10. Equation 2 was used for the calculation in Eq. (2):

$$T = \frac{K2}{In\left(\frac{K1}{L\lambda} + 1\right)} - 273.15 \quad (2)$$

where T is the temperature (Celsius), and K_2 and K_1 are the constant band(10). All information is obtained from the meta-data file of satellite images.

In the third step, normalized vegetation difference index (NDVI) analysis was performed after calculating the temperature degree. Bands 4 and 5 of the Landsat 8 satellite image were used in NDVI analyses as Eq. (3):

$$NDVI = \frac{(Band5 - Band4)}{(Band5 + Band4)} \quad (3)$$

where bands 4 and 5 are satellite images.

After performing the NDVI analysis, the vegetation cover rate is calculated. This value is made using NDVI analysis. Equation (4) was used to calculate the vegetation cover ratio:

$$PV = \left(\frac{(NDVI - NDVImin)}{(NDVImax - NDVImin)}\right)^2 \quad (4)$$

where PV is the vegetation rate, and NDVI is the NDVI analysis.

After calculating the vegetation cover ratio, LSE analysis was performed using Eq. (5). In addition, LST analysis was completed using Eq. (6):

$$\varepsilon = 0.004 * PV + 0.986 \quad (5)$$

Table 1 Dependent and explanatory variables used in the study

Category		Variables	Unit	Source	Spatial resolution
Dependent		Seasonal LST	°C	Landsat 8 OLI/TIRS	30*30 m
Explanatory	Vegetation	Seasonal normalized difference vegetation index	[0–1]	Landsat 8 OLI/TIRS	
	Natural structure	Elevation	m	DEM	1-ARC
	Land use type	Residential	%	CORINE, 2018	Sentinel 2 (10 m) Landsat (100 m)
		Commercial and industrial	%		
		Sport and leisure	%		
		Port areas	%		
		Forest	%		
		Water	%		
	Land use diversity	Entropy index	[0–1]		
	Transport	Railways	m	Extract.bbkike	
		Roads	m		
	Reflectance	Seasonal land surface albedo (LSA)	[0–1]	Landsat 8 OLI/TIRS	30*30 m
	Buildings	Number of buildings	Value	Extract.bbkike	
		Average building height	m		
	Population	Population density	Person/km^2	TUIK 2022	
		Mean age	Value		

where ε is the land surface emission, and PV is the vegetation ratio.

$$LST = \frac{T}{\left(1 + \frac{\lambda * T1}{c2}\right) * In(\varepsilon)} \tag{6}$$

where T is the temperature (Celsius), λ is the spectral radiance wavelength (Landsat 8 band10), c2 = h*c/s = 1.43888*10^{-2} mK = 14,388 mK, h is the Planck's constant: 6.626*10^{-34} J s, s is the Boltzmann constant = 1.38*10^{-23} J K, c is the velocity of light = 2.998*10^{8} m/s = 14,388, and ε is the LSE.

Normalized difference vegetation index (NDVI) and land surface albedo (LSA)

Sixteen variables explaining LST changes at the neighborhood scale were determined. Seasonal NDVI analysis, one of these variables, was calculated while making the LST map. Seasonal variation of LSA values was made using Landsat 8 OLI/TIRS satellite images in the ArcGIS 10.4.1. The following algorithm was used to perform LSA analysis in Eq. (7) (Kikon et al. 2016; Naegeli et al. 2017):

$$\alpha = (0.356\alpha 2 + 0.130\,\alpha 4 + 0.373\alpha 5 + 0.085\alpha 6 + 0.072\alpha 7 - 0.0018)/1.016 \tag{7}$$

where α is the albedo value, and α2,4,5,6,7 represents satellite image bands.

Urban morphology (UM)

Digital elevation model data provided by the United States Geological Survey (USGS) was used for elevation analysis. For land use analysis, CORINE data were digitally downloaded from the Copernicus Land Monitoring Service database, edited in the ArcGIS 10.4.1 program, and grouped into six classifications (residential, commercial, industrial, sport, and leisure areas, forest, and water areas).

The algorithm used to calculate the entropy index, which is an effective method for measuring land use diversity, is shown in Eq. (8) (Jeon et al. 2023):

$$\text{Entropy} = -\frac{\sum_j^k = 1\text{pj ln pj}}{\text{ln k}} \tag{8}$$

where p_j is the percentage of land use in the neighborhood unit, and k is the total number of land use classifications.

The values obtained at the end of the Entropy index vary between 0 and 1. Values close to 1 indicate the diversity of land use in that area. All variables used in the study were grouped at the neighborhood scale according to the (Jenks) method. It is preferred way because it provides more objective results in the classification of maps. The method is based on a statistical formula's natural grouping of data. This grouping helps to determine the differences between classes by grouping similar values.

The transportation data required within the scope of transportation was obtained from the Extract.bbkike (https://extract.bbbike.org/) database, which is an extension of Open Street. The ArcGIS program organized the data and grouped as railways and roads. Data regarding buildings, an important representation of UM, were obtained from the Extract.bbkike (https://extract.bbbike.org/) database, which is an extension of Open Street. The clip method was used in the ArcGIS 10.4.1 program to calculate the total number of buildings at the neighborhood scale.

The height data of the buildings were obtained from the Copernicus Land Monitoring Service database. The obtained elevation data were organized in the ArcGIS 10.4.1 program and classified into four groups representing the study area. Finally, the population data of the study area were obtained from the Turkish Statistical Institute (TUIK) database and transferred to the database created with the help of the ArcGIS 10.4.1 program.

Spatial analysis

OLS, a global regression method which is supported by regression analysis, was used to examine the correlation between LST values and the potential factors that may impact them. OLS is a linear regression model that models the relationship between the dependent and explanatory variables (Unsal et al. 2023).

Quadrant analysis

Quadrant analysis is considered a useful method for evaluating the current climatic situation and making effective planning decisions in the climate change process (Zhou et al. 2015; Ma et al. 2020). In quadrant analysis, the spatial distribution of the quadrants is effective in determining differences in terms of LULC and morphology. Using average LST values, quadrant analysis allows the study area to be classified in four categories according to the summertime (S) LST values on the axis and the intersection of the winter season (W) LST values on the y-axis in Fig. 2. There are four different quarters (Q1, Q2, Q3, and Q4) in the analysis. These quadrants are explained as follows (Jeon et al. 2023):

- Q1: Warmer LST values in S and W than in other regions,
- Q2: cooler LST values in S, warmer LST in W,
- Q3: cooler LST values in both S and W,
- Q4: the worst case of LST changes in regions with higher levels in S and colder degrees in W.

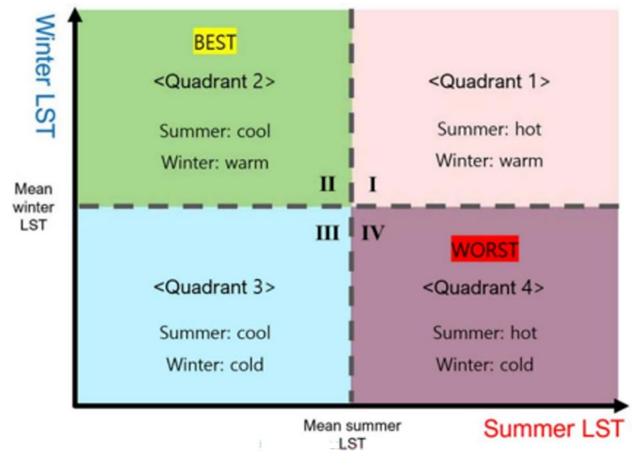

Fig. 2 Quadrant analysis matrix (Jeon et al. 2023)

Results

Seasonal variation of LST

Seasonal LST values of İzmir Konak district in 2023 were performed by Landsat 8 OLI-TIRS satellite image with 30 m spatial resolution. Looking at the seasonal LST maps, it is seen that the temperature values are between 55.95–60.84 °C in autumn and 47.20–52.30 °C in winter, while these values increase to 62.16–67.90 °C in spring and 64.43–71.18 °C in summer. LST values, which are the most important impact of climate change on cities, clearly show its impact in the study area. The 10.84 °C increase in temperature values in 8 months from the autumn to the summer season is an essential symptom of the impact of CC on coastal cities in Fig. 3.

Seasonal variation of normalized difference vegetation index (NDVI) and land surface albedo (LSA)

When looking at the seasonal NDVI change of Konak district, the lowest NDVI values are seen in autumn (− 0.01–0.05) and winter (− 0.01–0.04), while the highest NDVI value is seen in winter (0.35–1.00). When seasonal NDVI distribution maps are examined, it is seen that although there is an increase in the number of neighborhoods with NDVI concentration between the autumn and summer seasons, the highest NDVI values also decrease. This is an important indicator that the vegetation cover is weak in Fig. 4.

Looking at the seasonal LSA distribution maps of Konak district, although the highest LSA values are seen in the summer season (0.20–0.25), the number of neighborhoods with the highest LSA values is higher in the autumn season (0.15–0.19) (39 neighborhoods). The increase in LSA values from autumn to summer is an important indicator that the

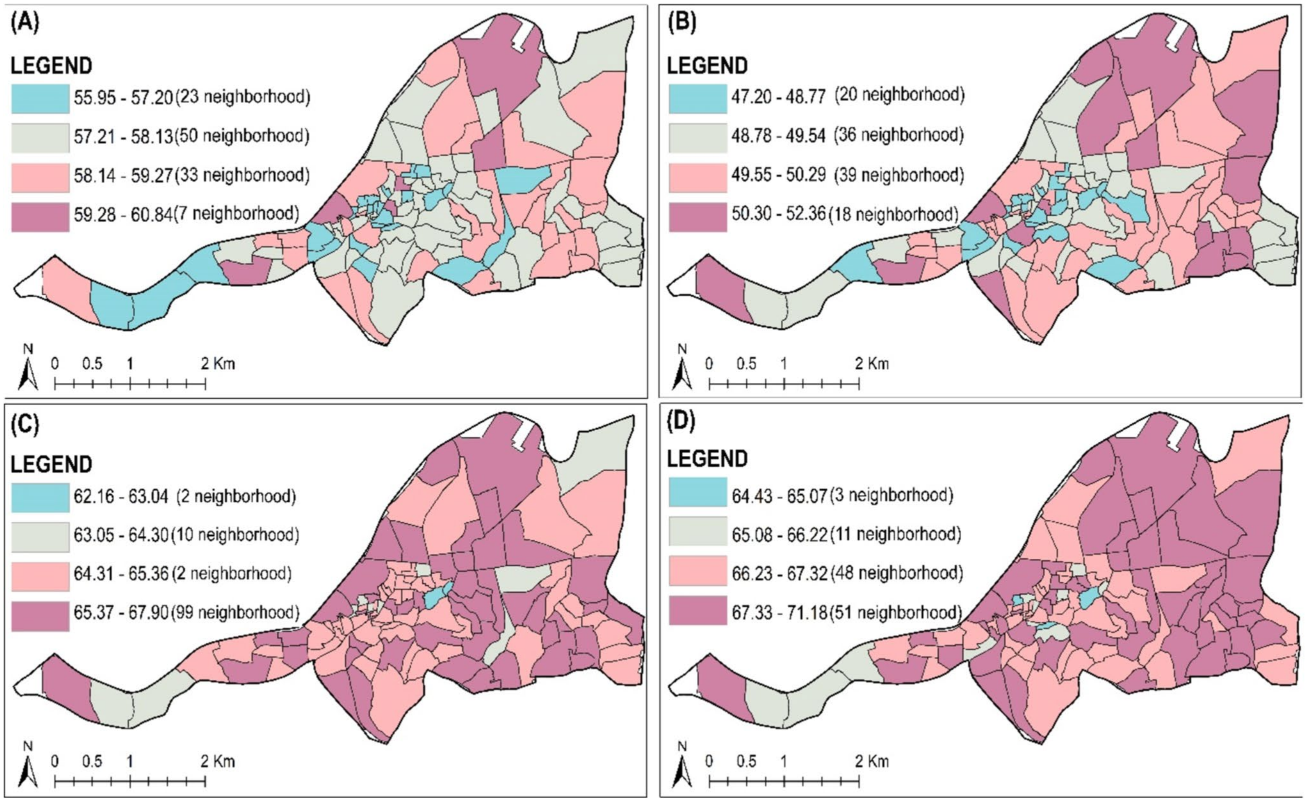

Fig. 3 Mean LST of Konak neighborhoods (**A** autumn, **B** winter, **C** spring, **D** summer)

surface reflectivity is high in the district. This is an effective parameter in reducing UHI formation by preventing the surface from heating. In this context, it is an essential indicator that the district has practical albedo values in Fig. 5.

Urban morphology features

Land uses and entropy index results

When looking at the elevation map of Konak district at the neighborhood scale, average heights mainly vary between − 11 and 82 m. It appears that the area generally has a flat land structure. Land use types were evaluated in 8 classes. According to this classification, approximately 75–100% of the area is residential. Percentage distribution maps of the neighborhoods were created for commercial and industrial areas, port areas, sports areas, forest areas, and water surfaces. Commercial, industrial and port area uses seem more prominent than other land use types. While there is mainly a 356 m railway in the neighborhoods of Konak district, it is seen that there is a road transportation connection up to 2696 m. According to the entropy index made according to land use types, it can be seen that the diversity value varies mainly between 0.27 and 0.65 in 38 neighborhoods in the Konak district in Fig. 6.

Buildings and population features

When the building and population variables are examined, there are mostly 599–1476 buildings in the neighborhoods of Konak district. The average height of these buildings varies between 9 and 20 m. When we look at the population density of the study area, it is seen that there is a density between 10.57 and 27.65 people/km^2, and the age of this population is predominantly 55 years old and above (Fig. 7).

Statistical analysis results

In the study, the association between LST and urban morphological features at the neighborhood scale was investigated by spatial regression and quadrant analysis using two analytical methods.

OLS modeling results

Four different OLS models were created according to seasonal distributions. While LST, NDVI, and LSA values were included in the analysis according to their seasonal

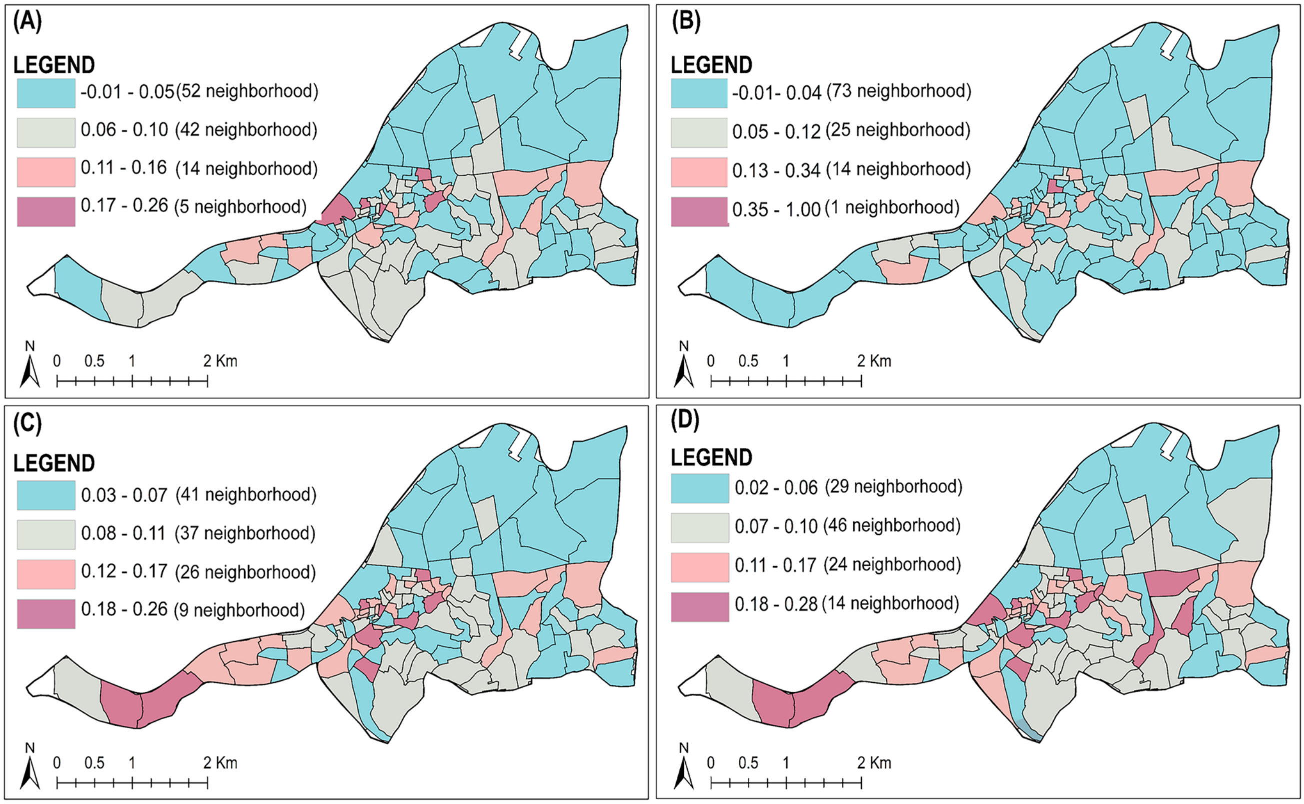

Fig. 4 Mean NDVI of Konak neighborhoods (**A** autumn, **B** winter, **C** spring, **D** summer)

distributions, other variables were used in 4 different OLS models (Table 2).

OLS model results show that the summer LST model showed the highest fit statistics, including R^2 and AICc values, all descriptive variables are statistically significant (SS), followed by the spring LST model. On the other hand, the winter LST model shows a lower model fit than other seasons. Winter temperatures are harder to describe on the basis of UM indices such as vegetation cover, land use, building and population characteristics. The summer months are subject to the most significant temperature exposure from urban areas, both natural and artificial surroundings. Model results are given in Table 3. The OLS model for the autumn season shows that the variables in the study area explain approximately 26% of the LST values, with an Akaike's Information Criterion (AICc) value of 294.12 and an adjusted R^2 value of 0.26.

In addition, findings show that the descriptive factors are SS ($p<0.01$ and $p<0.05$). OLS results show a negative relationship between elevation, NDVI, LSA, forest area, sport and leisure, water areas, entropy index, and LST. A positive relationship exists between residential, commercial, and industrial port areas, railways, roads, number of buildings, average building height, population density mean age, and LST.

The OLS model for the winter season shows that the variables in the study area explain approximately 31% of the LST values, with an Akaike's Information Criterion (AICc) value of 265.05 and an R^2 value of 0.31. In addition, the results show that the explanatory variables are SS ($p<0.01$ and $p<0.05$). According to OLS results, a negative relationship exists between NDVI, elevation, sport and leisure, forest, water areas, entropy index, railways and roads, and LST. In contrast, there is a positive relationship between density and mean age and LST in LSA, residential, commercial, and industrial port areas, number of buildings, average building height, and population.

The spring season OLS model shows that the study area variables explain approximately 34% of the LST values, with an Akaike's Information Criterion (AICc) value of 250.75 and an R^2 value of 0.34. OLS results for the spring season also show that the explanatory variables are SS ($p<0.01$ and $p<0.05$). According to the OLS model results, while there is a negative relationship between elevation, NDVI, LSA, sport and leisure, forest, water areas and entropy index and LST values, residential, commercial and industrial, port area, railways, roads, number of buildings, average building There is a positive relationship between height, population density and mean age and LST.

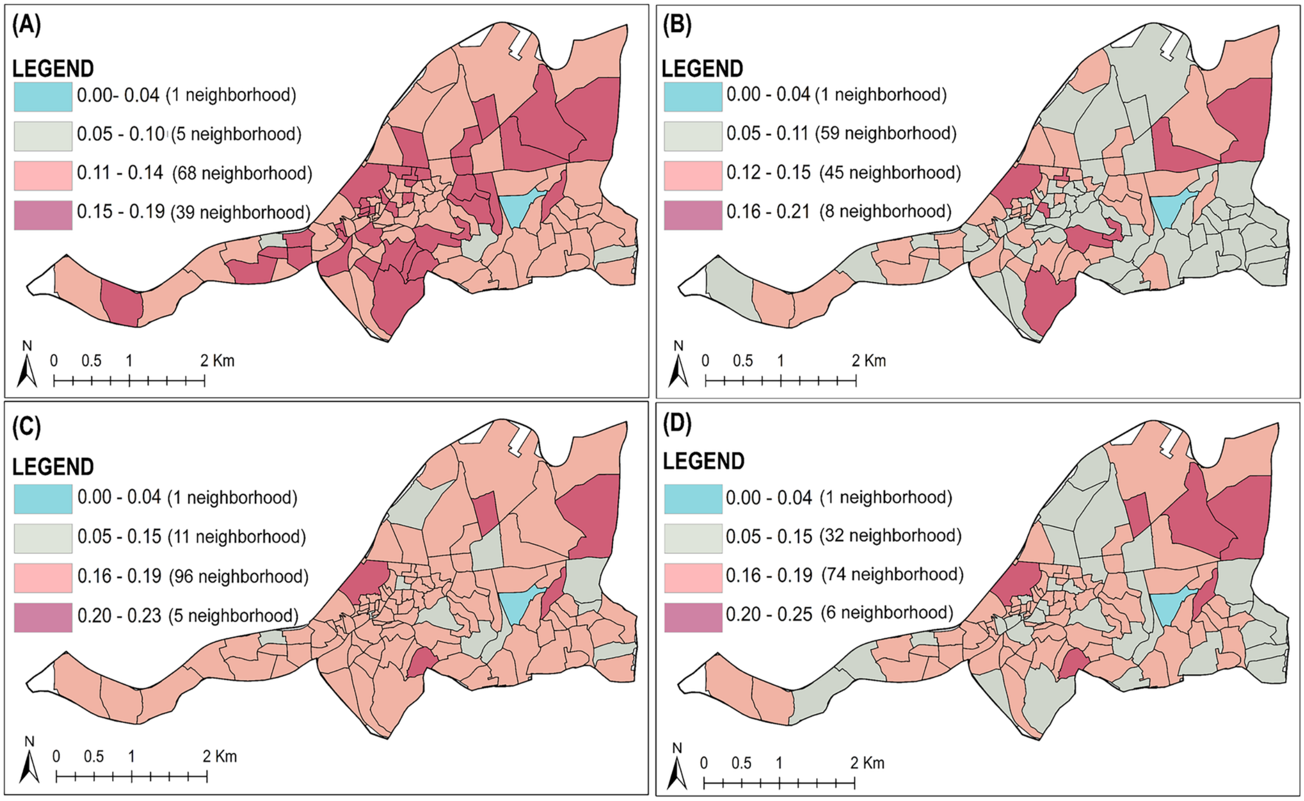

Fig. 5 Mean LSA of Konak neighborhoods (**A** autumn, **B** winter, **C** spring, **D** summer)

The OLS model for the summer season shows that the variables in the study area explain approximately 43% of the LST values, with an Akaike's Information Criterion (AICc) value of 339.67 and an R^2 value of 0.43. As in other OLS models, the results show that the explanatory variables are SS ($p < 0.01$ and $p < 0.05$). According to the model results, it shows that there is a negative relationship between elevation, NDVI, LSA, forest, water areas and entropy index and LST values, residential, commercial and industrial, sport and leisure, port areas, railways, roads, number of buildings, average building height, and population. It shows that there is a positive relationship between density and mean age and LST values.

Moran's I statistic was calculated to analyze the spatial distribution of residual values of OLS models. The results show that the autocorrelation of the OLS models is significant, and the residual values are spatially clustered. These values also show that the OLS model contributes to predicting the relationship between explanatory variables and LST on a local scale in Table 4.

Quadrant analysis results

Konak district neighborhoods were divided into four quadrants using the average summer LST (67.28 °C) and average winter LST (49.54 °C). The first quadrant represents the higher LST in both summer and winter, and the third represents the lower LST in both seasons. The second quadrant is preferred as it represents the cooler summer and warmer winter LST. The 4th quarter represents the least preferred section with hotter summer and colder winter temperatures.

According to the quadrant analysis given in Fig. 8, the highest number of neighborhoods (80) are in the 3rd quarter, followed by the 1st quarter (20 neighborhoods). There are only 10 neighborhoods in the 2nd quarter. The quadrant analysis for Konak district is an important indicator that the district has consistently warmer or colder LST values in both summer and winter compared to other regions.

Following is the spatial distribution of the four different quadrants in 113 neighborhoods of Konak district shows notable clustering along with spatial inequalities in the number of neighborhoods in the quarters (Moran's I: 0.10, *z*-score: 3.76, *p*-value: 0.00).

Comparing the mean values of explanatory variables according to the characteristics of each quarter provides more information in Table 5. Q4 has the highest vegetation density (NDVI: 0.13) in the study area. It also has the highest values in terms of height (74.33 m) and commercial and industrial (17.95%). Q4 does not include sports and leisure, port areas, forest, water, and railways areas.

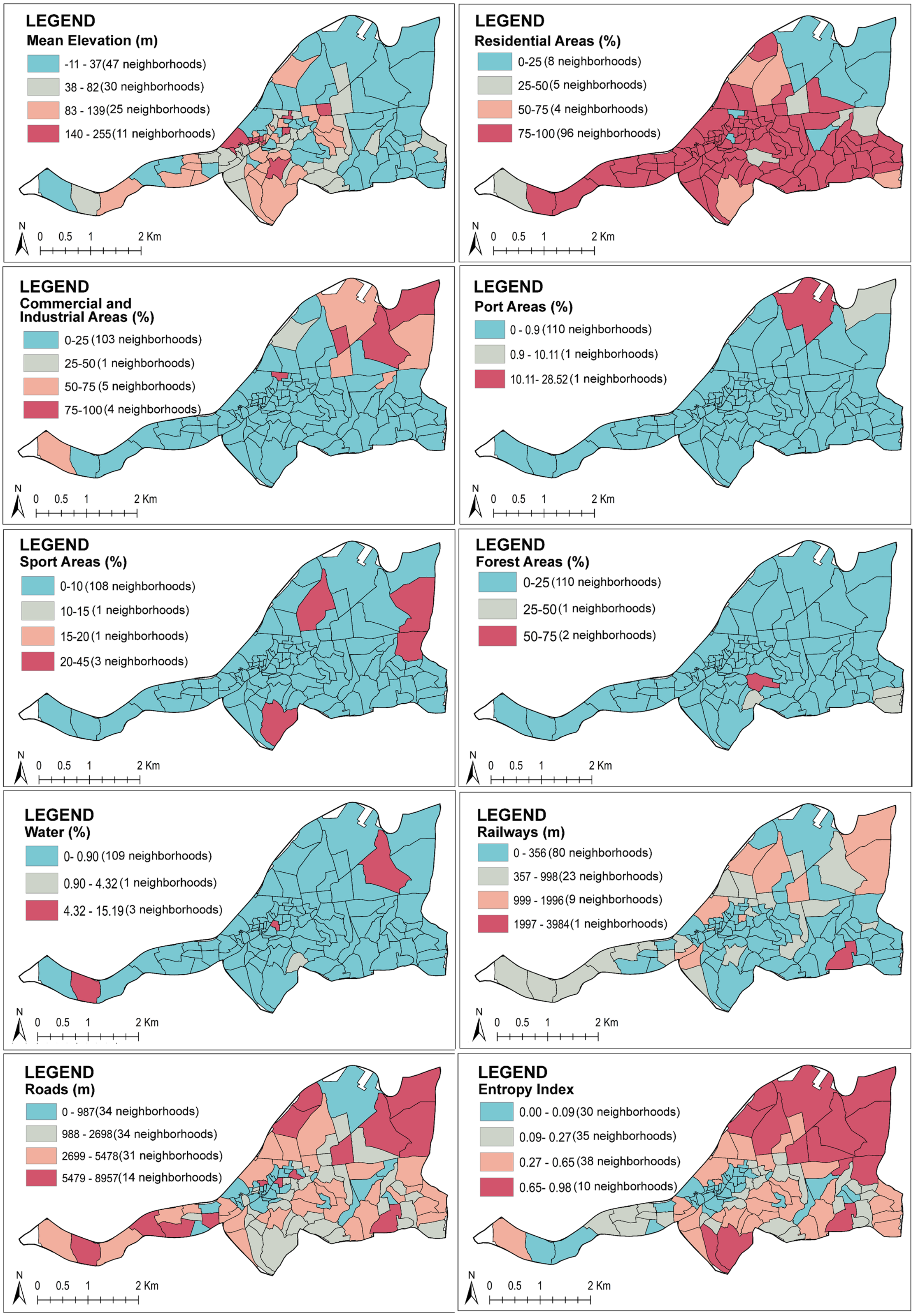

Fig. 6 LULC and entropy index of Konak neighborhoods

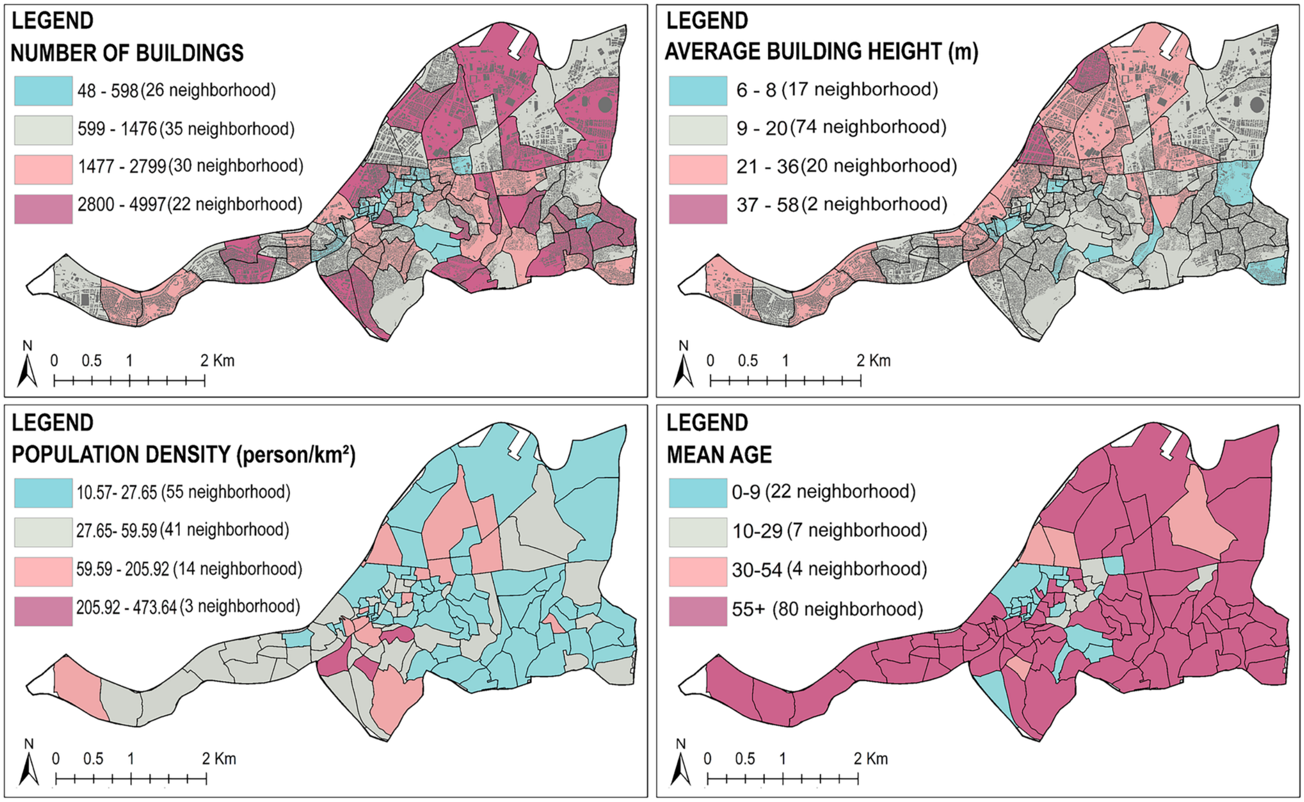

Fig. 7 Building and population variables of Konak neighborhoods

Discussion

Along with urbanization, population growth, and the global developments that come with it, urban areas have higher temperatures due to various activities such as transportation and trade. These high temperatures also increase the formation of UHI. Increasing the combat power of urban areas is an important necessity in the process of climate change, which is one of the biggest environmental problems in the world today. LULC changes occurring in cities cause significant changes in the temperature differences in the city and its surroundings (Logan et al. 2020; Yang et al. 2020). These temperature differences are also the main reasons for the formation of UHI (Wang et al. 2015; Peng et al. 2016; Li et al. 2017; Yao et al. 2022). Since the formation of UHI is directly related to the geometry of cities, urban growth increases surface temperatures and the level of heat stress experienced by people. Many studies show that urban form characteristics are among the most fundamental factors affecting the formation of UHI (Heaviside et al. 2016; Ward et al. 2016; Liang et al. 2020). Some studies are focusing on the role of green areas, especially in reducing UHI formation in the process of combating climate change. In these studies, green areas, which have many environmental benefits, are considered one of the most effective methods to reduce the UHI effect. Within the scope of this study, the relationship between the morphological features that can be intervened in the process of combating ST and the basic built environment parameters affecting this relationship were focused on. In general, the results obtained are similar to the literature. However, since UHI studies conducted especially at the neighborhood scale are limited in number (Mostofi et al. 2021; Shi et al. 2021; Yang et al. 2023), the study has important findings in this respect.

Influences of UM on seasonal LST

In the study, the seasonal LST and morphological features of Konak district of Izmir, one of the important coastal cities of Turkey, were revealed to be interrelated with OLS models. Since urban morphological features significantly impact seasonal LST, it is vital to determine the extent of these effects (Chen et al. 2023; Han et al. 2022, 2023). In studies conducted on similar subjects in the literature, OLS model results (R^2) generally vary between 0.23 and 0.73. These values are among the acceptable values for urban morphology studies (Huang et al. 2019; Li et al. 2020; Sun et al. 2020b; Kashki et al. 2021). The R^2 values obtained within the scope of the study were also calculated in a close range with the studies in the literature (autumn: 0.26, winter:

Table 2 Defining statistical analysis of LST and the explanatory statistics

Category	Variable		Mean	Std. dev	Min	Max
LST	LST (°C)	Autumn	57.90	0.85	55.95	60.84
		Winter	49.54	0.77	47.20	52.36
		Spring	65.16	0.80	62.26	67.90
		Summer	67.28	1.06	64.43	71.18
Vegetation	NDVI	Autumn	0.07	0.04	− 0.01	0.26
		Winter	0.07	0.19	− 0.01	1.00
		Spring	0.10	0.05	0.03	0.26
		Summer	0.10	0.05	0.02	0.28
Reflectance	LSA	Autumn	0.13	0.02	0.00	0.19
		Winter	0.11	0.02	0.00	0.21
		Spring	0.16	0.02	0.00	0.23
		Summer	0.16	0.02	0.00	0.25
UM	Natural structure	Elevation (m)	64	56	− 11	255
	Land use proportion (%)	Residential	87.76	27.07	0	100
		Commercial and industrial	7.12	21.38	0	100
		Sport and leisure	1.34	7.23	0	45.98
		Port areas	0.34	2.82	0	28.52
		Forest	2.27	10.24	0	75.38
		Water	0.39	2.01	0	15.19
	Land use diversity	Entropy index	0.29	0.27	0.00	1.25
	Transport (m)	Railways	336	610	0	3984
		Roads	2576	2348	0	8957
	Buildings	Number of buildings	1654	1257	48	4997
		Average building height (m)	16	8	6	58
	Population	Population density (person/km^2)	44.11	63.95	10.57	473.64

0.31, spring: 0.34, summer: 0.43). Statistically, the differences between explanatory variables and LST values are more remarkable in spring and summer than in autumn and winter. OLS results also show that the dominant factors are more substantial in summer and weaker in winter. This result is consistent with the results of other studies in the literature (Hu et al. 2020; Li et al. 2021). At the same time, the effect of explanatory variables on LST values is not absolute and decreases with the decrease in average temperature (Chen et al. 2019).

It is imperative to include building characteristics when assessing UM. The number of buildings and building heights in neighborhoods also have a dominant role in LST (Berger et al. 2017; Chen et al. 2022). High building heights are expected to cause lower temperatures due to the shadow effect and the creation of wind vents that direct colder air to the streets (Hwang et al. 2011; Zheng et al. 2019). However, this study concluded a positive relationship between building heights and seasonal LST values. DEM data of the study area were used to examine the relationship between LST and topographic conditions. The OLS model confirmed a negative relationship between the elevation of the area and seasonal LST values, which result is consistent with Peng et al. (2018).

The presence of high LST values in areas with dense construction in the study area is consistent with the results of other papers in the literature (Kafy et al. 2021; Liao et al. 2021; Hong and Heo 2023). It is an essential indicator of the impact of built environments on LST. In addition, it was concluded that there is a significant inverse connection between the entropy index and LST as an expression of diversity in land use. In general, Konak district exhibits a lower correlation between LST and urban morphological variables compared to other places (Kelly Turner et al. 2022; Hong and Heo 2023).

Effects of vegetation on seasonal LST

The relationship between NDVI and LST values in Konak district is negative. Areas with the highest NDVI values have lower LST, while areas with weak vegetation have higher values of LST. This result is also compatible with Singh et al. (2018) and Chun and Guldmann (2018). Vegetation is a natural air conditioning system that supports the formation of cool air in the atmosphere by absorbing solar radiation and the transpiration of water through the leaves. Therefore, NDVI is one of UHIs' most critical physical determinants. The effect of vegetation on LST varies seasonally. This effect

Table 3 OLS model results

Variable	Autumn	Winter	Spring	Summer
NDVI	− 0.34*	− 0.66**	− 3.43**	− 6.84*
LSA	− 0.45*	4.20**	− 2.61**	2.17**
Elevation (m)	− 0.03**	− 0.02**	− 0.00**	− 0.01*
Residential	0.00*	0.01*	0.00*	0.00**
Commercial and industrial	0.00*	0.00*	0.00*	0.05*
Sport and leisure	− 0.00**	− 0.00**	− 0.01*	0.00*
Port areas	0.02**	0.00*	0.05*	0.08**
Forest	− 0.02*	− 0.01*	− 0.00*	− 0.01*
Water	− 0.04**	− 0.03**	− 0.03*	− 0.03**
Entropy index	− 0.76*	− 0.67*	− 0.95*	− 0.76*
Railways	0.00**	− 0.00**	0.00*	0.01*
Roads	0.00**	− 0.00**	0.00*	0.01*
Number of buildings	0.00*	0.00*	0.00**	0.00**
Average building height (m)	0.00*	0.00*	0.01**	0.00**
Population density	0.00*	0.00*	0.00*	0.00*
Mean age	0.04**	0.04**	0.00*	0.02*
Adjusted R^2	0.26	0.31	0.34	0.43
AIC_c	294.12	265.05	250.75	339.67

*p-value < 0.01

**p-value < 0.05

Table 4 Moran I statistical results

OLS model	Moran I	z-score	p-value
Autumn	0.19	6.85	0.00
Winter	0.24	8.82	0.00
Spring	0.13	4.85	0.00
Summer	0.25	9.32	0.00

$p < 0.01$

is expected to be more intense, especially in spring and summer. The vegetation's effect on LST values was revealed with OLS models. As a result of the model results, it was concluded that the most excellent effect was in the summer months. This result is equivalent to the results of Zhou et al. (2014).

Effects of population on seasonal LST

Consistent with the literature, it was concluded that LST values increased with the increase in population density in Konak district (Weng et al. 2008; Kotharkar et al. 2016; Huang et al. 2016). Findings show that most neighborhoods have a good correlation among the population aged 55 and over and LST values. This result is inconsistent with Unsal et al. (2023). However, based on the positive relationship between average age and LST, according to the OLS model results, it is possible to say dependent population and LST are inversely correlated. While the LST values increase as the average age level increases, and LST values decrease as the average age level decreases.

Conclusion

The CC is predicted to cause extreme climate phenomena such as extreme HW and colder weather periods beyond expectations. Therefore, it is vital to build the ability of cities and societies through effective urban planning decisions to adapt to these inter-seasonal temperature changes. The present research explored the seasonal correlation between urban temperature variations and UM at the neighborhood scale in Konak district of Izmir, one of the most important coastal cities of Türkiye. Quadrant analysis revealed spatial separation between areas highly adapted to LST (CSM and WWN) and susceptible to LST (warmer summers (WSM) and CWN). At the same time, significant differences were found between vegetation, UM, and LST. Seasonal variables of urban landscape and constructed form are analyzed with OLS models under spatial regression studies to determine the seasonal effects of urban landscape and constructed form variables on LST. Higher NDVI plays an essential role in mitigating LST. It makes summers cooler and winters warmer. Building and population characteristics also have a seasonally stable effect on LST. According to the entropy index as a representation of diversity in land use, a higher land use mix has a seasonally significant effect on reducing LST. These findings obtained within the study's scope are valid for analyses conducted at the neighborhood scale. These findings are essential in that they reveal the intense pressure of population and urbanization on LST and the effect of vegetation on mitigating LST.

Holistic planning approaches are needed to consider the role of GCT on sustainable development, particularly megacities. It includes the need to include LST data in urban planning, the adoption of technologies and innovations in energy efficiency, the promotion of green infrastructure in all cities, the development of human health measures to be more efficient and effective, and the need to prioritize CC adaptation and mitigation strategies. Cities should be developed to create healthier, livable, resilient and sustainable urban environments, taking into account the nexus of LST and sustainable development.

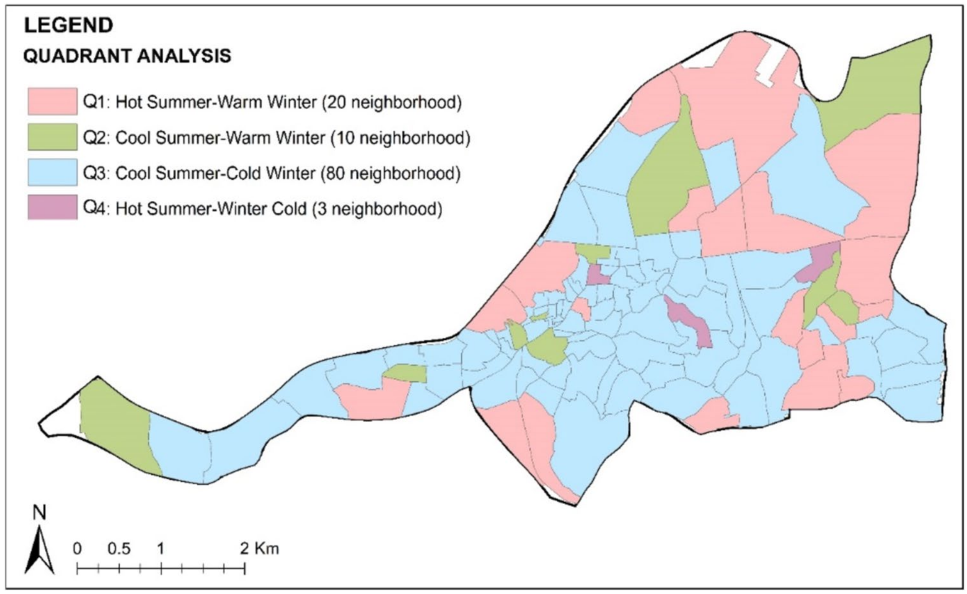

Fig. 8 Spatial pattern of the summer–winter LST quadrants in Konak

Table 5 Average quartile statistics of LST and explanatory variables

Category	Variable		Q1	Q2	Q3	Q4
LST	LST (°C)	Autumn	59.07	58.38	57.50	59.09
		Winter	50.53	50.26	49.22	48.92
		Spring	65.96	64.15	64.8	65.03
		Summer	68.88	67.49	68.84	68.40
Vegetation	NDVI	Autumn	0.07	0.05	0.07	0.11
		Winter	0.08	0.06	0.05	0.12
		Spring	0.09	0.08	0.11	0.12
		Summer	0.09	0.08	0.10	0.13
Reflectance	LSA	Autumn	0.13	0.14	0.13	0.11
		Winter	0.11	0.12	0.11	0.09
		Spring	0.16	0.17	0.16	0.16
		Summer	0.16	0.17	0.16	0.16
UM	Natural structure	Elevation (m)	45.05	60.05	68.68	74.33
	Land use proportion (%)	Residential	78.48	69.70	92.56	82.04
		Commercial and industrial	11.17	25.36	3.42	17.95
		Sport and leisure	3.35	3.89	0.56	0
		Port areas	1.42	1.01	0.01	0
		Forest	4.97	0	1.97	0
		Water	0.50	0.02	0.40	0
	Land use diversity	Entropy index	0.48	0.37	0.25	0.14
	Transport (m)	Railways	562.45	581.2	261.275	0
		Roads	3794.45	3080.1	2252.363	1406.33
	Buildings	Number of buildings	2672	1496	1455	675.66
		Average building height (m)	19.1	16.7	14.92	11.33
	Population	Population density (person/km^2)	29.25	57.83	46.84	24.51
		Mean age	55 +	50–54	35–39	35.39

Limitations and future research directions

Firstly, this research properly present the climate and urban characteristics of the study area and state that the results are applicable only to cities with similar conditions. It suffers from various limitations, first: the thermal data are LST values observed at 08:52 am for all seasons. Additional efforts are required to explore the feasibility of implementation parameters to spatial LST changes at other points in time before or after 08:52. Second, some variables were not taken into account due to data limitations. For instance, more precise spatial scale building geometry calculations such as SVF values and building surface areas are impossible. There is also a need to determine the impact of variables at building scale such as building alignment and height-to-width ratio on LST. Third, this study only considered the total length of railways and roads within the scope of vehicle and pedestrian traffic, significantly affecting LST. However, anthropogenic heat emissions due to transportation were not taken into account. E Individual aspects of building forms can trigger emissions of dissimilar wastes. These anthropogenic issues demand more investigation. Finally, while the present paper aims to address the spatial relationship among LST and urban morphological variables, these relationships may differ at different scales in different cities. It is thought that this potential situation may be a subject worth researching in the future.

Acknowledgements Not applicable.

Author contributions Oznur Isinkaralar: conceptualization, methodology, validation, formal analysis, visualization, investigation, data curation, writing—original draft, writing—reviewing and editing. Kaan Isinkaralar: conceptualization, writing—reviewing and editing. Dilara Yilmaz: validation, formal analysis, investigation, data curation, writing—original draft, writing—reviewing and editing. Sevgi Öztürk: data curation, writing—reviewing and editing.

Funding There is no financial support and commercial support.

Data availability The data that support the findings of this study are available from the corresponding author, upon reasonable request.

Declarations

Conflict of interest The authors declare that they have no conflict of interest.

Ethics approval All the authors have read, understood, and have complied as applicable with the statement on "Ethical responsibilities of Authors" as found in the Instructions for Authors.

Consent to participate Not applicable.

Consent to publish Not applicable.

References

Adams MP, Smith PL (2014) A systematic approach to model the influence of the type and density of vegetation cover on urban heat using remote sensing. Landsc Urban Plan 132:47–54. https://doi.org/10.1016/j.landurbplan.2014.08.008

Ayanlade A, Aigbiremolen MI, Oladosu OR (2021) Variations in urban land surface temperature intensity over four cities in different ecological zones. Sci Rep 11(1):20537. https://doi.org/10.1038/s41598-021-99693-z

Aydin H, Yenigun K, Isinkaralar O, Isinkaralar K (2024) Hydrological low flow and overlapped trend analysis for drought assessment in Western Black Sea Basin. Nat Hazards 1–31. https://doi.org/10.1007/s11069-024-06880-y

Barsi JA, Lee K, Kvaran G, Markham BL, Pedelty JA (2014) The spectral response of the landsat-8 operational land imager. Remote Sens 6(10):10232–10251. https://doi.org/10.3390/rs61010232

Berger C, Rosentreter J, Voltersen M, Baumgart C, Schmullius C, Hese S (2017) Spatio-temporal analysis of the relationship between 2D/3D urban site characteristics and land surface temperature. Remote Sens Environ 193:225–243. https://doi.org/10.1016/j.rse.2017.02.020

Boeing G (2018) Measuring the complexity of urban form and design. Urban Des Int 23(4):281–292. https://doi.org/10.1057/s41289-018-0072-1

Bokaie M, Zarkesh MK, Arasteh PD, Hosseini A (2016) Assessment of urban heat island based on the relationship between land surface temperature and land use/land cover in Tehran. Sustain Cities Soc 23:94–104. https://doi.org/10.1016/j.scs.2016.03.009

Chen J, Chu R, Wang H, Zhang L, Chen X, Du Y (2019) Alleviating urban heat island effect using high-conductivity permeable concrete pavement. J Clean Prod 237:117722. https://doi.org/10.1016/j.jclepro.2019.117722

Chen J, Zhan W, Du P, Li L, Li J, Liu Z, Huang F, Lai J, Xia J (2022) Seasonally disparate responses of surface thermal environment to 2D/3D urban morphology. Build Environ 214:108928. https://doi.org/10.1016/j.buildenv.2022.108928

Chen Y, Yang J, Yu W, Ren J, Xiao X, Xia JC (2023) Relationship between urban spatial form and seasonal land surface temperature under different grid scales. Sustain Cities Soc 89:104374. https://doi.org/10.1016/j.scs.2022.104374

Choudhury D, Das K, Das A (2019) Assessment of land use land cover changes and its impact on variations of land surface temperature in asansol-durgapur development region. Egyptian J Remote Sens Space Sci 22(2):203–218. https://doi.org/10.1016/j.ejrs.2018.05.004

Chun B, Guldmann JM (2018) Impact of greening on the urban heat island: seasonal variations and mitigation strategies. Comput Environ Urban Syst 71:165–176. https://doi.org/10.1016/j.compenvurbsys.2018.05.006

Dai Z, Guldmann JM, Hu Y (2018) Spatial regression models of park and land use impacts on the Urban heat Island in central Beijing. Sci Total Environ 626:1136–1147. https://doi.org/10.1016/j.scitotenv.2018.01.165

Deilami K, Kamruzzaman M, Liu Y (2018) Urban heat island effect: a systematic review of spatio-temporal factors, data, methods, and mitigation measures. Int J Appl Earth Obs Geoinf 67:30–42. https://doi.org/10.1016/j.jag.2017.12.009

Dimoudi A, Nikolopoulou M (2003) Vegetation in the urban environment: microclimatic analysis and benefits. Energy Build 35(1):69–76. https://doi.org/10.1016/S0378-7788(02)00081-6

Elmes A, Rogan J, Williams C, Ratick S, Nowak D, Martin D (2017) Effects of urban tree canopy loss on land surface temperature magnitude and timing. ISPRS J Photogramm Remote Sens 128:338–353. https://doi.org/10.1016/j.isprsjprs.2017.04.011

Estoque RC, Murayama Y (2014) Measuring sustainability based upon various perspectives: a case study of a hill station in Southeast Asia. Ambio 43:943–956. https://doi.org/10.1007/s13280-014-0498-7

Estoque RC, Murayama Y, Myint SW (2017) Effects of landscape composition and pattern on land surface temperature: an urban heat island study in the megacities of Southeast Asia. Sci Total Environ 577:349–359. https://doi.org/10.1016/j.scitotenv.2016.10.195

Ferwati S, Skelhorn C, Shandas V, Makido Y (2019) A comparison of neighborhood-scale interventions to alleviate urban heat in Doha. Qatar Sustain 11(3):730. https://doi.org/10.3390/su11030730

Firozjaei MK, Kiavarz M, Alavipanah SK, Lakes T, Qureshi S (2018) Monitoring and forecasting heat island intensity through multitemporal image analysis and cellular automata-Markov chain modelling: a case of Babol city. Iran Ecol Indic 91:155–170. https://doi.org/10.1016/j.ecolind.2018.03.052

Guo A, Yang J, Sun W, Xiao X, Cecilia JX, Jin C, Li X (2020a) Impact of urban morphology and landscape characteristics on spatiotemporal heterogeneity of land surface temperature. Sustain Cities Soc 63:102443. https://doi.org/10.1016/j.scs.2020.102443

Guo A, Yang J, Xiao X, Xia J, Jin C, Li X (2020b) Influences of urban spatial form on urban heat island effects at the community level in China. Sustain Cities Soc 53:101972. https://doi.org/10.1016/j.scs.2019.101972

Guo B, Wang Y, Pei L, Yu Y, Liu F, Zhang D, Wang X, Su Y, Zhang D, Zhang B, Guo H (2021) Determining the effects of socioeconomic and environmental determinants on chronic obstructive pulmonary disease (COPD) mortality using geographically and temporally weighted regression model across Xi'an during 2014–2016. Sci Total Environ 756:143869. https://doi.org/10.1016/j.scitotenv.2020.143869

Guo F, Schlink U, Wu W, Hu D, Sun J (2023) Scale-dependent and season-dependent impacts of 2D/3D building morphology on land surface temperature. Sustain Cities Soc. https://doi.org/10.1016/j.scs.2023.104788

Guven DS, Yenigun K, Isinkaralar O, Isinkaralar K (2024) Modeling flood hazard impacts using GIS-based HEC-RAS technique towards climate risk in Şanlıurfa, Türkiye. Nat Hazards 1–19. https://doi.org/10.1007/s11069-024-06945-y

Han D, An H, Wang F, Xu X, Qiao Z, Wang M, Sui X, Liang S, Hou X, Cai H, Liu Y (2022) Understanding seasonal contributions of urban morphology to thermal environment based on boosted regression tree approach. Build Environ 226:109770. https://doi.org/10.1016/j.buildenv.2022.109770

Han S, Hou H, Estoque RC, Zheng Y, Shen C, Murayama Y, Pan J, Wang B, Hu T (2023) Seasonal effects of urban morphology on land surface temperature in a three-dimensional perspective: a case study in Hangzhou. China Build Environ 228:109913. https://doi.org/10.1016/j.buildenv.2022.109913

He BJ, Zhu J, Zhao DX, Gou ZH, Qi JD, Wang J (2019a) Co-benefits approach: opportunities for implementing sponge city and urban heat island mitigation. Land Use Policy 86:147–157. https://doi.org/10.1016/j.landusepol.2019.05.003

He J, Zhao W, Li A, Wen F, Yu D (2019b) The impact of the terrain effect on land surface temperature variation based on landsat-8 observations in mountainous areas. Int J Remote Sens 40(5–6):1808–1827. https://doi.org/10.1080/01431161.2018.1466082

Heaviside C, Vardoulakis S, Cai XM (2016) Attribution of mortality to the urban heat island during heatwaves in the West Midlands, UK. Environ Health 15:49–59. https://doi.org/10.1186/s12940-016-0100-9

Hong T, Heo Y (2023) Exploring the impact of urban factors on land surface temperature and outdoor air temperature: a case study in Seoul. Korea Build Environ 243:110645. https://doi.org/10.1016/j.buildenv.2023.110645

Hornsey MJ, Fielding KS (2020) Understanding (and reducing) inaction on climate change. Soc Issues Policy Rev 14(1):3–35. https://doi.org/10.1111/sipr.12058

Hu Y, Dai Z, Guldmann JM (2020) Modeling the impact of 2D/3D urban indicators on the urban heat island over different seasons: a boosted regression tree approach. J Environ Manage 266:110424. https://doi.org/10.1016/j.jenvman.2020.110424

Huang G, Cadenasso ML (2016) People, landscape, and urban heat island: dynamics among neighborhood social conditions, land cover and surface temperatures. Landscape Ecol 31:2507–2515. https://doi.org/10.1007/s10980-016-0437-z

Huang Y, Yuan M, Lu Y (2019) Spatially varying relationships between surface urban heat islands and driving factors across cities in China. Environ Planning B: Urban Analytics City Sci 46(2):377–394. https://doi.org/10.1177/2399808317716935

Hwang RL, Lin TP, Matzarakis A (2011) Seasonal effects of urban street shading on long-term outdoor thermal comfort. Build Environ 46(4):863–870. https://doi.org/10.1016/j.buildenv.2010.10.017

Imran HM, Hossain A, Islam AS, Rahman A, Bhuiyan MAE, Paul S, Alam A (2021) Impact of land cover changes on land surface temperature and human thermal comfort in Dhaka city of Bangladesh. Earth Syst Environ 5:667–693. https://doi.org/10.1007/s41748-021-00243-4

IPCC (The Intergovernmental Panel on Climate Change) (2022) Climate Change 2022. https://www.ipcc.ch/report/ar6/wg2/

IPCC (The Intergovernmental Panel on Climate Change) (2023) AR6 synthesis report: Climate change 2023. https://www.ipcc.ch/report/ar6/syr/

Isinkaralar O, Isinkaralar K, Sevik H, Küçük Ö (2024a) Spatial modeling the climate change risk of river basins via climate classification: a scenario-based prediction approach for Türkiye. Nat Hazards 120(1):511–528. https://doi.org/10.1007/s11069-023-06220-6

Isinkaralar O, Sharifi A, Isinkaralar K (2024b) Assessing spatial thermal comfort and adaptation measures for the Antalya basin under climate change scenarios. Clim Change 177(8):118. https://doi.org/10.1007/s10584-024-03781-8

Jeon G, Park Y, Guldmann JM (2023) Impacts of Urban morphology on seasonal land surface temperatures: comparing grid-and block-based approaches. ISPRS Int J Geo Inf 12(12):482. https://doi.org/10.3390/ijgi12120482

Kafy AA, Shuvo RM, Naim MNH, Sikdar MS, Chowdhury RR, Islam MA et al (2021) Remote sensing approach to simulate the land use/land cover and seasonal land surface temperature change using machine learning algorithms in a fastest-growing megacity of Bangladesh. Remote Sens Appl: Soc Environ 21:100463. https://doi.org/10.1016/j.rsase.2020.100463

Kashki A, Karami M, Zandi R, Roki Z (2021) Evaluation of the effect of geographical parameters on the formation of the land surface temperature by applying OLS and GWR, a case study Shiraz City. Iran Urban Climate 37:100832. https://doi.org/10.1016/j.uclim.2021.100832

Kelly Turner V, Rogers ML, Zhang Y, Middel A, Schneider FA, Ocón JP, Seeley M, Dialesandro J (2022) More than surface temperature: mitigating thermal exposure in hyper-local land system. J Land Use Sci 17(1):79–99. https://doi.org/10.1080/1747423X.2021.2015003

Kikon N, Singh P, Singh SK, Vyas A (2016) Assessment of urban heat islands (UHI) of Noida City, India using multi-temporal satellite data. Sustain Cities Soc 22:19–28. https://doi.org/10.1016/j.scs.2016.01.005

Kotharkar R, Surawar M (2016) Land use, land cover, and population density impact on the formation of canopy urban heat islands through traverse survey in the Nagpur urban area, India. J Urban

Plann Develop 142(1):04015003. https://doi.org/10.1061/(ASCE)UP.1943-5444.0000277
Li J, Song C, Cao L, Zhu F, Meng X, Wu J (2011) Impacts of landscape structure on surface urban heat islands: a case study of Shanghai. China Remote Sens Environ 115(12):3249–3263. https://doi.org/10.1016/j.rse.2011.07.008
Li W, Cao Q, Lang K, Wu J (2017) Linking potential heat source and sink to urban heat island: heterogeneous effects of landscape pattern on land surface temperature. Sci TotalEnviron 586:457–465. https://doi.org/10.1016/j.scitotenv.2017.01.191
Li L, Zha Y, Zhang J (2020) Spatially non-stationary effect of underlying driving factors on surface urban heat islands in global major cities. Int J Appl Earth Obs Geoinf 90:102131. https://doi.org/10.1016/j.jag.2020.102131
Li H, Li Y, Wang T, Wang Z, Gao M, Shen H (2021) Quantifying 3D building form effects on urban land surface temperature and modeling seasonal correlation patterns. Build Environ 204:108132. https://doi.org/10.1016/j.buildenv.2021.108132
Liang Z, Wu S, Wang Y, Wei F, Huang J, Shen J, Li S (2020) The relationship between urban form and heat island intensity along the urban development gradients. Sci Total Environ 708:135011. https://doi.org/10.1016/j.scitotenv.2019.135011
Liao W, Hong T, Heo Y (2021) The effect of spatial heterogeneity in urban morphology on surface urban heat islands. Energy Build 244:111027. https://doi.org/10.1016/j.enbuild.2021.111027
Liu W, Meng Q, Allam M, Zhang L, Hu D, Menenti M (2021) Driving factors of land surface temperature in urban agglomerations: a case study in the pearl river delta, china. Remote Sens 13(15):2858. https://doi.org/10.3390/rs13152858
Liu X, Ming Y, Liu Y, Yue W, Han G (2022) Influences of landform and urban form factors on urban heat island: comparative case study between Chengdu and Chongqing. Sci Total Environ 820:153395. https://doi.org/10.1016/j.scitotenv.2022.153395
Liu B, Guo X, Jiang J (2023) How Urban morphology relates to the Urban heat Island effect: a multi-indicator study. Sustainability 15(14):10787. https://doi.org/10.3390/su151410787
Logan TM, Zaitchik B, Guikema S, Nisbet A (2020) Night and day: the influence and relative importance of urban characteristics on remotely sensed land surface temperature. Remote Sens Environ 247:111861. https://doi.org/10.1016/j.rse.2020.111861
Lu L, Weng Q, Xiao D, Guo H, Li Q, Hui W (2020) Spatiotemporal variation of surface urban heat islands in relation to land cover composition and configuration: a multi-scale case study of Xi'an. China Remote Sensing 12(17):2713. https://doi.org/10.3390/rs12172713
Ma L, Liu S, Fang F, Che X, Chen M (2020) Evaluation of urban-rural difference and integration based on quality of life. Sustain Cities Soc 54:101877. https://doi.org/10.1016/j.scs.2019.101877
Martin M, Ramani V, Miller C (2024) InfraRed Investigation in Singapore (IRIS) observatory: Urban heat island contributors and mitigators analysis using neighborhood-scale thermal imaging. Energy Build 307:113973. https://doi.org/10.1016/j.enbuild.2024.113973
Meng Q, Zhang L, Sun Z, Meng F, Wang L, Sun Y (2018) Characterizing spatial and temporal trends of surface urban heat island effect in an urban main built-up area: A 12-year case study in Beijing, China. Remote Sens Environ 204:826–837. https://doi.org/10.1016/j.rse.2017.09.019
Moazzam MFU, Doh YH, Lee BG (2022) Impact of urbanization on land surface temperature and surface urban heat Island using optical remote sensing data: a case study of Jeju Island. Repub Korea Build Environ 222:109368. https://doi.org/10.1016/j.buildenv.2022.109368
Mostofi N, Aghamohammadi Zanjirabad H, Vafaeinejad A, Ramezani M, Hemmasi A (2021) Developing an SDSS for optimal sustainable roof covering planning based on UHI variation at neighborhood scale. Environ Monit Assess 193(6):372. https://doi.org/10.1007/s10661-021-09151-6
Naegeli K, Damm A, Huss M, Wulf H, Schaepman M, Hoelzle M (2017) Cross-comparison of albedo products for glacier surfaces derived from airborne and satellite (sentinel-2 and landsat 8) optical data. Remote Sens 9(2):110. https://doi.org/10.3390/rs9020110
Nastran M, Kobal M, Eler K (2019) Urban heat islands in relation to green land use in European cities. Urban For Urban Green 37:33–41. https://doi.org/10.1016/j.ufug.2018.01.008
Oke TR, Mills G, Christen A, Voogt JA (2017) Urban climates. Cambridge University Press
Park H, Song J (2023) Relationship between flood damage and flood vulnerability focusing on property damage and human casualties. J Korea Plann Association 58(3):149–166. https://doi.org/10.1720/jkpa.2023.06.58.3.149
Parsaee M, Joybari MM, Mirzaei PA, Haghighat F (2019) Urban heat island, urban climate maps and urban development policies and action plans. Environ Technol Innov 14:100341. https://doi.org/10.1016/j.eti.2019.100341
Peng J, Xie P, Liu Y, Ma J (2016) Urban thermal environment dynamics and associated landscapepattern factors: a case study in the Beijing metropolitan region. Remote Sens Environ 173:145–155. https://doi.org/10.1016/j.rse.2015.11.027
Peng J, Ma J, Liu Q, Liu Y, Li Y, Yue Y (2018) Spatial-temporal change of land surface temperature across 285 cities in China: an urban-rural contrast perspective. Sci Total Environ 635:487–497. https://doi.org/10.1016/j.scitotenv.2018.04.105
Qi L, Hu Y, Bu R, Li B, Gao Y, Li C (2024) Evaluation of the thermal environment based on the Urban neighborhood heat/cool Island effect. Land 13(7):933. https://doi.org/10.3390/land13070933
Ren J, Yang J, Zhang Y, Xiao X, Xia JC, Li X, Wang S (2022) Exploring thermal comfort of urban buildings based on local climate zones. J Clean Prod 340:130744. https://doi.org/10.1016/j.jclepro.2022.130744
Roy S, Pandit S, Eva EA, Bagmar MSH, Papia M, Banik L et al (2020) Examining the nexus between land surface temperature and urban growth in chattogram metropolitan area of Bangladesh using long term landsat series data. Urban Clim 32:100593. https://doi.org/10.1016/j.uclim.2020.100593
Shi Y, Liu S, Yan W, Zhao S, Ning Y, Peng X et al (2021) Influence of landscape features on urban land surface temperature: Scale and neighborhood effects. Sci Total Environ 771:145381. https://doi.org/10.1016/j.scitotenv.2021.145381
Shiflett SA, Liang LL, Crum SM, Feyisa GL, Wang J, Jenerette GD (2017) Variation in the urban vegetation, surface temperature, air temperature nexus. Sci Total Environ 579:495–505. https://doi.org/10.1016/j.scitotenv.2016.11.069
Singh VK, Singh BP, Kisi O, Kushwaha DP (2018) Spatial and multidepth temporal soil temperature assessment by assimilating satellite imagery, artificial intelligence and regression based models in arid area. Comput Electron Agric 150:205–219. https://doi.org/10.1016/j.compag.2018.04.019
Song J, Chen W, Zhang J, Huang K, Hou B, Prishchepov AV (2020) Effects of building density on land surface temperature in China: spatial patterns and determinants. Landsc Urban Plan 198:103794. https://doi.org/10.1016/j.landurbplan.2020.103794
Sun F, Liu M, Wang Y, Wang H, Che Y (2020a) The effects of 3D architectural patterns on the urban surface temperature at a neighborhood scale: relative contributions and marginal effects. J Clean Prod 258:120706. https://doi.org/10.1016/j.jclepro.2020.120706
Sun Y, Wang S, Wang Y (2020b) Estimating local-scale urban heat island intensity using nighttime light satellite imageries. Sustain Cities Soc 57:102125. https://doi.org/10.1016/j.scs.2020.102125

Tan J, Yu D, Li Q, Tan X, Zhou W (2020) Spatial relationship between land-use/land-cover change and land surface temperature in the Dongting Lake area. China Scientific Rep 10(1):9245. https://doi.org/10.1038/s41598-020-66168-6

Tanoori G, Soltani A, Modiri A (2024) Machine learning for Urban heat Island (UHI) analysis: predicting land surface temperature (LST) in Urban environments. Urban Clim 55:101962. https://doi.org/10.1016/j.uclim.2024.101962

Unsal Ö, Lotfata A, Avci S (2023) Exploring the relationships between land surface temperature and its influencing determinants using local spatial modeling. Sustainability 15(15):11594. https://doi.org/10.3390/su151511594

Wang J, Huang B, Fu D, Atkinson PM (2015) Spatiotemporal variation in surface urban heat island intensity and associated determinants across major Chinese cities. Remote Sens 7(4):3670–3689. https://doi.org/10.3390/rs70403670

Wang Y, Yi G, Zhou X, Zhang T, Bie X, Li J, Ji B (2021) Spatial distribution and influencing factors on urban land surface temperature of twelve megacities in China from 2000 to 2017. Ecol Ind 125:107533. https://doi.org/10.1016/j.ecolind.2021.107533

Ward K, Lauf S, Kleinschmit B, Endlicher W (2016) Heat waves and urban heat islands in Europe: a review of relevant drivers. Sci Total Environ 569:527–539. https://doi.org/10.1016/j.scitotenv.2016.06.119

Weng Q, Lu D, Schubring J (2004) Estimation of land surface temperature–vegetation abundance relationship for urban heat island studies. Remote Sens Environ 89(4):467–483. https://doi.org/10.1016/j.rse.2003.11.005

Weng Q, Liu H, Liang B, Lu D (2008) The spatial variations of urban land surface temperatures: pertinent factors, zoning effect, and seasonal variability. IEEE J Sel Top Appl Earth Observations Remote Sens 1(2):154–166. https://doi.org/10.1109/JSTARS.2008.917869

WHO (World Health Organization) (2014) Quantitative risk assessment of the effects of climate change on selected causes of death, 2030s and 2050s. World Health Organization

Wu J (2010) Urban sustainability: an inevitable goal of landscape research. Landsc Ecol 25:1–4. https://doi.org/10.1007/s10980-009-9444-7

Xin J, Yang J, Sun D, Han T, Song C, Shi Z (2022) Seasonal differences in land surface temperature under different land use/land cover types from the perspective of different climate zones. Land 11(8):1122. https://doi.org/10.3390/land11081122

Yang J, Zhan Y, Xiao X, Xia JC, Sun W, Li X (2020) Investigating the diversity of land surface temperature characteristics in different scale cities based on local climate zones. Urban Clim 34:100700. https://doi.org/10.1016/j.uclim.2021.100937

Yang J, Shi Q, Menenti M, Wong MS, Wu Z, Zhao Q, Abbas S, Xu Y (2021) Observing the impact of urban morphology and building geometry on thermal environment by high spatial resolution thermal images. Urban Clim 39:100937. https://doi.org/10.1016/j.uclim.2021.100937

Yang Y, Xu Y, Duan Y, Zhang S, Zhang Y, Xie Y (2023) How can trees protect us from air pollution and urban heat? associations and pathways at the neighborhood scale. Landsc Urban Plan 236:104779. https://doi.org/10.1016/j.landurbplan.2023.104779

Yao L, Yang X, Zhu C, Jin T, Peng LL, Ye Y (2017) Evaluation of a diagnostic equation for the daily maximum urban heat island effect. Procedia Eng 205:2863–2870. https://doi.org/10.1016/j.proeng.2017.09.911

Yao L, Sun S, Song C, Wang Y, Xu Y (2022) Recognizing surface urban heat 'island'effect and itsurbanization association in terms of intensity, footprint, and capacity: a case study with multi- dimensional analysis in Northern China. J Clean Prod 372:133720. https://doi.org/10.1016/j.jclepro.2022.133720

Yin C, Yuan M, Lu Y, Huang Y, Liu Y (2018) Effects of urban form on the urban heat island effect based on spatial regression model. Sci Total Environ 634:696–704. https://doi.org/10.1016/j.scitotenv.2018.03.350

Yuan F, Bauer ME (2007) Comparison of impervious surface area and normalized difference vegetation index as indicators of surface urban heat island effects in landsat imagery. Remote Sens Environ 106(3):375–386. https://doi.org/10.1016/j.rse.2006.09.003

Yuan B, Zhou L, Hu F, Wei C (2024) Effects of 2D/3D urban morphology on land surface temperature: contribution, response, and interaction. Urban Clim 53:101791. https://doi.org/10.1016/j.uclim.2023.101791

Zhang N, Xiong K, Xiao H, Zhang J, Shen C (2023) Ecological environment dynamic monitoring and driving force analysis of karst world heritage sites based on remote-sensing: a case study of Shibing Karst. Land 12(1):184. https://doi.org/10.3390/land12010184

Zhao L, Li T, Przybysz A, Liu H, Zhang B, An W, Zhu C (2023a) Effects of urban lakes and neighbouring green spaces on air temperature and humidity and seasonal variabilities. Sustain Cities Soc 91:104438. https://doi.org/10.1016/j.scs.2023.104438

Zhao Y, Sen S, Susca T, Iaria J, Kubilay A, Gunawardena K et al (2023b) Beating urban heat: multimeasure-centric solution sets and a complementary framework for decision-making. Renew Sustain Energy Rev 186:113668. https://doi.org/10.1016/j.rser.2023.113668

Zheng Z, Zhou W, Yan J, Qian Y, Wang J, Li W (2019) The higher, the cooler? effects of building height on land surface temperatures in residential areas of Beijing. Phys Chem Earth Parts a/b/c 110:149–156. https://doi.org/10.1016/j.pce.2019.01.008

Zhou D, Zhao S, Liu S, Zhang L, Zhu C (2014) Surface urban heat island in China's 32 major cities: spatial patterns and drivers. Remote Sens Environ 152:51–61. https://doi.org/10.1016/j.rse.2014.05.017

Zhou J, Zhang X, Shen L (2015) Urbanization bubble: four quadrants measurement model. Cities 46:8–15. https://doi.org/10.1016/j.cities.2015.04.007

Zhou D, Xiao J, Bonafoni S, Berger C, Deilami K, Zhou Y et al (2018) Satellite remote sensing of surface urban heat islands: progress, challenges, and perspectives. Remote Sens 11(1):48. https://doi.org/10.3390/rs11010048

Zhou Y, Zhao H, Mao S, Zhang G, Jin Y, Luo Y et al (2022) Exploring surface urban heat island (SUHI) intensity and its implications based on urban 3D neighborhood metrics: an investigation of 57 Chinese cities. Sci Total Environ 847:157662. https://doi.org/10.1016/j.scitotenv.2022.157662